



Studies on the Mechanism of Interaction of Congo Red with Lysozyme by Spectroscopic Methods

X.H. LI, X.H. LU, J.P. LIANG*, Z.J. XIN and X. ZHOU

Institute of Modern Physics, Chinese Academy of Sciences, Lanzhou 730000, P.R. China

*Corresponding author: Fax:+ 98 931 2115287; Tel: +98 931 4969698, E-mail: lixh@impcas.ac.cn

(Received: 12 July 2012;

Accepted: 30 April 2013)

AJC-13422

Interaction between Congo red and lysozyme was investigated by spectroscopic methods. The analysis of fluorescence data indicated the presence of both dynamic and static quenching mechanism in the binding of Congo red with lysozyme. Various binding parameters have been evaluated. The circular dichroism measurements revealed the conformational changes of lysozyme from α -helix to distorted helix structure thereby indicating the conformational change in lysozyme upon binding. The thermodynamic data showed that hydrophobic interactions playing a major role in Congo red binding to lysozyme.

Key Words: Binding, Congo red, Lysozyme, Fluorescence, Circular dichroism.

INTRODUCTION

Dyes are being increasingly used for clinical and medicinal purposes¹. The discovery of some dyes would stain certain tissues and not others led to the idea that dyes might destroy pathogenic organisms without causing appreciable harm to the host. Congo red, chemically, 3, 3'-[(1,1'-biphenyl)-4,4'-diylbis(azo)]-bis-(4-amino-1-naphthalene acid) disodium salt, is a symmetrical linear molecule (Fig. 1). Congo red is potentially toxic. It can reduce serum protein concentration and cause platelet aggregation, thrombocytopenia and disseminated microembolism^{2,3}. Given orally, Congo red is cleaved by enzymes present in the mammalian gut, intestines or liver, delivering benzidine, a highly carcinogenic compound, known to induce hepatocellular and urinary bladder carcinomas⁴⁻⁷. In addition, experimental analyses have shown that Congo red has teratogenic properties^{8,9}.

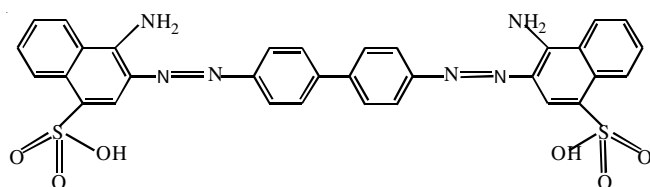


Fig. 1. Structure of Congo red

Lysozyme, a small monomeric globular protein, consists of 129 amino acid residues and contains six tryptophan and three tyrosine residues¹⁰. With a molecular weight of about 14,306, its tertiary structure is compact with several helices

surrounding a small β -sheet region. Since lysozyme was recognized by Fleming in 1922 as a bacteriolytic agent having an ability to hydrolyze bacterial cell walls, it has become one of the most intensively studied proteins. The action of lysozyme on bacteria works cooperatively and synergistically with antibiotics, which has a very important practical value in medicinal area. Moreover, tryptophan or tyrosine residues can cure abscess, stomatitis, rheum, *etc. via* binding to antibiotics. Therefore, studies on the interaction between Congo red and lysozyme are of importance in view of realizing disposition, transportation and metabolism of dye as well as efficacy process involving dye and lysozyme. A large amount of results have been published for the interaction of dye with proteins^{11,12}. Yet, few results have been involved in dye binding to lysozyme.

In this work, we will report our studies on the interaction of Congo red with lysozyme by excitation-emission matrix fluorescence, steady fluorescence, resonance light scanning fluorescence, UV-VIS absorption and circular dichroism measurements. Efforts were made to investigate the quenching mechanism, binding constants, binding sites, binding mode and the effect of Congo red on the conformation of lysozyme.

EXPERIMENTAL

Lysozyme was purchased from Shanghai Institute of Biochemistry and Cell Biology, Chinese Academy of Sciences. The concentration of lysozyme was determined spectrophotometrically on a Shimadzu UV-260 UV-vis spectrophotometer using $A_{280\text{ nm}}(1\%) = 2.64^{13}$. All stock solutions of

2.5 μM lysozyme were prepared with pH 7.40 (20 mM sodium phosphate). AnalaR grade Congo red was used in the study. The stock solution of 1.5 mM Congo red was prepared by dissolving it in double-distilled water. All other reagents were of analytical grade. Double-distilled water was used throughout all experiments.

All fluorescence spectra were recorded on LS-55 spectrofluorimeter (Perkin Elmer, America) equipped with 1.0 cm quartz cells and thermostat bath. Both excitation and emission slit widths were adjusted at 10 nm.

Fluorometric experiments: 3.0 mL Solution containing appropriate concentration of lysozyme was titrated by successive additions of stock solution of Congo red. Titrations were done manually by using trace syringes and the fluorescence intensity was measured (excitation at 280 nm) over a wavelength range of 300-500 nm.

Three-dimensional spectra were obtained by measuring the emission spectra, in the range 300-550 nm, repeatedly, at excitation wavelengths from 200 to 340 nm, spaced by 10 nm intervals in the excitation domain. Fully corrected spectra were then concatenated into an excitation-emission matrix. Three dimensional plots and contour maps of total luminescence spectra were produced using origin program. All contour maps were plotted using the same scale range of fluorescence intensities.

The resonance light scattering fluorescence spectra were collected by simultaneously scanning the excitation and emission monochromator. By scanning the wavelength interval ($\Delta\lambda$) with 0 nm, a resonance light scanning spectrum has been proved to be able to investigate the aggregation of small molecules and the long-range assembly of organic dyes on biological templates¹⁴. All resonance light scanning spectra were obtained from 250 to 600 nm.

UV absorption spectra were measured on a Shimadzu UV-260 UV-VIS spectrophotometer in a 1 cm cuvette. Absorption spectra were recorded over a wavelength range of 190-300 nm. Circular dichroism spectra were recorded on an Olis DSM-1000 automatic recording spectropolarimeter (USA) over the range of 200-250 nm in a 1 mm cell equipped with a temperature controlling unit. Each circular dichroism spectrum given was an average of three scans at 298 K.

RESULTS AND DISCUSSION

Fluorescence contour plots of the excitation-emission matrix for lysozyme in the absence and presence of Congo red: The fluorescence contour plots of the excitation-emission matrix for lysozyme in the absence and presence of Congo red was observed (Fig. 2). Three-dimensional spectra were obtained by excitation in the range of 200-340 nm and emission in the range of 300-500 nm. The optimal excitation wavelength was centred at $\lambda_{\text{ex}}/\lambda_{\text{em}} = 280/347$ nm. In the same way, the optimal excitation wavelength was obtained at 320 nm for Congo red. After the addition of Congo red, the location of fluorescence maxima slightly shifted and the fluorescence intensity decreased dramatically. The fluorescence contour plots for the mixture of lysozyme and Congo red showed there were interactions between the compounds and overlapping among their spectra. In this diagram, it is easy to select the

optimal excitation wavelength for further investigations of this complex mixture.

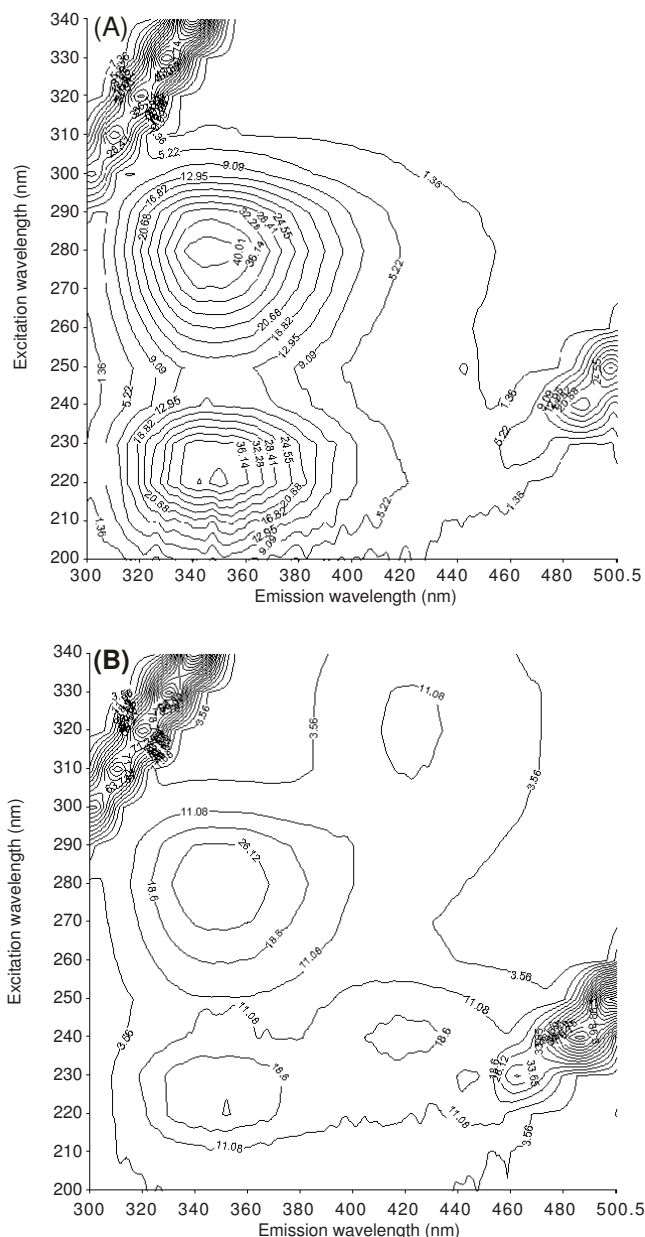


Fig. 2. Fluorescence contour plots for lysozyme (A), the mixture of lysozyme and Congo red (B)

Fluorescence emission of lysozyme in the presence of Congo red: The more comprehensive data concerning change of lysozyme with various amounts of Congo red following an excitation at 280 nm were achieved from the emission spectra. As Fig. 3 shows, lysozyme exhibits a strong fluorescence emission band at 347 nm. Its intensity decreased gradually with the addition of Congo red, *i.e.*, the excited lysozyme was quenched by Congo red. It was also observed that an increase in the fluorescence intensity at 417 nm assigned to Congo red, which was well observed at the fluorescence contour plots of the excitation-emission matrix. These observations may be referred to a strong binding of Congo red to lysozyme and a radiationless energy transfer between Congo red and lysozyme¹⁵. Furthermore, an isoactinic point at 418 nm was

observed in Fig. 3. It indicated the existence of both bound and free Congo red at equilibrium¹⁶.

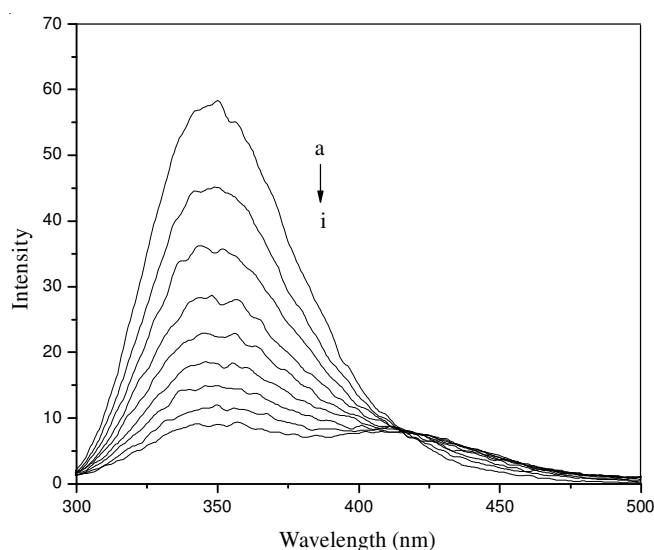


Fig. 3. Fluorescence emission spectra of: lysozyme (2.5 μM) with various amounts of Congo red: 0 (a), 2.5 (b), 5 (c), 7.5 (d), 10 (e), 12.5 (f), 15 (g), 17.5 (h) and 20 μM (i), at pH 7.40

The fluorescence quenching data are analyzed with the Stern-Volmer equation (eqn. 1)¹⁷:

$$\frac{F_0}{F} = 1 + K_{SV}[Q] \quad (1)$$

where F_0 and F are the relative fluorescence intensities in the absence and presence of quencher, respectively, $[Q]$ is the concentration of quencher, K_{SV} the Stern-Volmer quenching constant. The plot of F_0/F for lysozyme versus $[Q]$ of Congo red (Fig. 4) showed positive deviation (concave towards the y axis) indicating the presence of both static and dynamic quenching process¹⁸. The fluorescence data were further examined using modified Stern-Volmer equation:

$$\frac{F_0}{F_0 - F} = \frac{1}{fK_{SV}[Q]} + \frac{1}{f} \quad (2)$$

where f is the fraction of the initial fluorescence which is accessible to the quencher and K_{SV} is the Stern-Volmer quenching constant. From the plot of $F_0/(F_0 - F)$ versus $1/[Q]$ (Fig. 5), the values of f and K_{SV} were obtained from the values of intercept and slope, respectively. The values of ' f ' were observed to be 1.47 and the K_{SV} were found to be $6.71 \times 10^5 \text{ M}^{-1}$. The rate constant for the bimolecular quenching process, k_q was evaluated using the equation, $k_q = K_{SV}/\tau_0$. Where τ_0 is the average bimolecular life-time in the absence of quencher evaluated at about 5 ns¹⁹. So the values of k_q were observed to be $1.34 \times 10^{13} \text{ LM}^{-1}\text{S}^{-1}$.

In fact, in many cases, fluorophores can be quenched by both collision and complex formation with the same quencher. Consequently, the Stern-Volmer plot will exhibit an upward curve, being concave towards the y-axis at higher $[Q]$ ²⁰ (Fig. 4). Accordingly, F_0/F is related to $[Q]$ by the following modified form (eqn. 3) of the Stern-Volmer equation²¹:

$$\frac{F_0}{F} = (1 + K_D[Q])(1 + K_S[Q]) \quad (3)$$

where K_D and K_S are the dynamic and static quenching constants, respectively. It is second order in $[Q]$ and thus leads to upward curve plots of F_0/F versus $[Q]$ at higher $[Q]$ arising from a combined quenching (both dynamic and static) process.

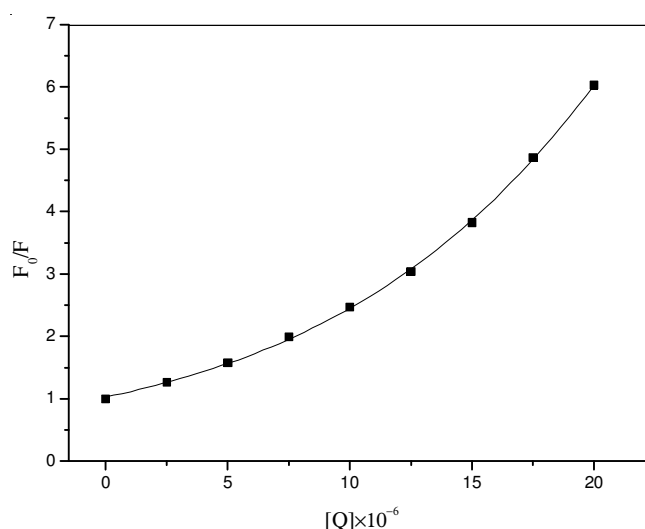


Fig. 4. Stern-Volmer plots for the binding of Congo red to lysozyme at pH 7.40 (■)

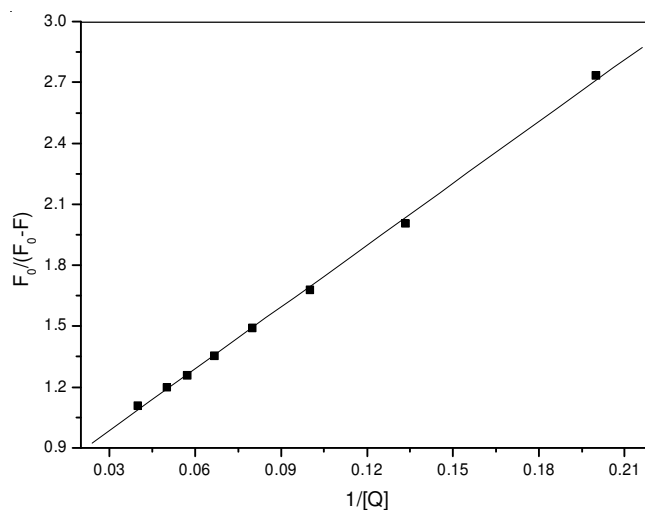


Fig. 5. Modified Stern-Volmer plots for the binding of Congo red to lysozyme at pH 7.40 (■)

Evaluation of the binding constant and binding site of lysozyme with Congo red: When small molecules are bound independently to a set of equivalent sites on a macromolecule, the equilibrium between free and bound molecules is given by eqn. (4)²²:

$$\log \frac{F_0 - F}{F} = \log K + n \log [Q] \quad (4)$$

where K is the binding constant and n the number of binding sites. Thus, the values for K and n can be derived from the intercept and slope of plots of $\log(F_0 - F)/F$ versus $\log [Q]$. The value for K was observed to be $21.067 \times 10^5 \text{ LM}^{-1}$ and the value for n was also found to be 1.23, respectively. The value for K shows that there exist a strong interaction between Congo red and lysozyme.

The binding interaction force between lysozyme and Congo red: Intermolecular interacting forces between a small

molecule and biomacromolecule include hydrogen bond, van der Waals force, electrostatic and hydrophobic interactions, *etc.* Thermodynamic parameters for a binding interaction can be used as a major evidence to learn the nature of intermolecular forces. Thus, the temperature-dependent thermodynamic parameters for the Congo red-lysozyme system are used to characterize the intermolecular forces between Congo red and lysozyme. The enthalpy change ΔH° and entropy change ΔS° for a binding reaction can be derived from the van't Hoff equations (Eqs. 5 and 6):

$$\ln K = -\frac{\Delta H^\circ}{RT} + \frac{\Delta S^\circ}{R} \quad (5)$$

$$\Delta G^\circ = \Delta H^\circ - T\Delta S^\circ \quad (6)$$

where K is the binding constant at the corresponding temperature and R the gas constant. The enthalpy change ΔH° and entropy change ΔS° were obtained from the slope and intercept of the linear van't Hoff plot of $\ln K$ versus $1/T$ based on eqn. (5). The free energy change ΔG° was estimated from eqn. (6). The fluorescence quenching experiment of lysozyme by Congo red was carried out at 293 K and 308 K. The negative value of ΔG° ($-513.14 \text{ J mol}^{-1}$ and $-554.41 \text{ J mol}^{-1}$) reveals that the binding process is a spontaneous process. The positive ΔS° ($2.75 \text{ J mol}^{-1} \text{ K}^{-1}$) change arises from water molecules arranged more random around lysozyme and dye, caused by hydrophobic interactions between lysozyme and Congo red. Besides, the positive ΔH° ($293.04 \text{ J mol}^{-1}$) is considered as another evidence for hydrophobic interactions. Thus, positive values for both ΔH° and ΔS° indicate hydrophobic interactions playing a major role in Congo red binding to lysozyme²³.

The enhancement of resonance light scattering is always associated with the aggregation and depends sensitively on the electronic properties of the individual chromophores. Lysozyme has one strong resonance light scattering peaks at 392 nm (Fig. 6). It is evident that the fluorescence intensity of lysozyme increased regularly with the variation of Congo red concentration, indicating that the interaction between lysozyme and Congo red has occurred. Since the enhancement of resonance light scattering is always associated with the aggregation and depends sensitively on the electronic properties of the individual chromophores, so it is reasonable to establish the aggregation mechanism of the Congo red at the surface of lysozyme.

Analysis of the conformation of lysozyme upon addition of Congo red

UV-visible spectroscopic studies on Congo red binding to lysozyme: Fig. 7 shows the UV absorption spectra of lysozyme and lysozyme-Congo red (1:5). The addition of Congo red led to increase in the lysozyme absorbance and a little red shift. These observations can be rationalized in terms of interactions between Congo red and lysozyme in the ground state and formation of a ground state complex²⁴. The slight shift of the peaks also indicate that the peptide strands of lysozyme molecules are much extended with the addition of Congo red and the hydrophobicity of lysozyme was diminished²⁵.

Circular dichroism spectroscopic studies on Congo red binding to lysozyme: The circular dichroism data directly relate to the conformation of the protein. The negative ellipticity bands at 208 and 222 nm of circular dichroism spectra of lysozyme are characteristic of the amount of α -helix in the

protein and changes in the spectra at these wavelengths may reflect the shifts in the α -helical content of the protein. In Fig. 8, the circular dichroism spectrum of free lysozyme in buffer solution had a characteristic of the typical α -helix structure with negative bands at 207 and 225 nm. After interacting with Congo red, the band intensity of negative cotton effect of lysozyme at 207 and 225 nm reduced, indicating the considerable changes in the protein secondary structure with the decrease of the α -helical content in lysozyme. This could mean that Congo red provided different chiral environments for lysozyme. When the Congo red concentration in lysozyme microemulsion increased, the spectrum showed a significant change from the α -helical to distortion helical structure. From the above results, it may be suggested the formation of complex between Congo red and lysozyme in microemulsion. At the same time, the intramolecular forces responsible for maintaining the secondary and tertiary structures can be altered, resulting in a conformational change of the protein when Congo red binds to lysozyme.

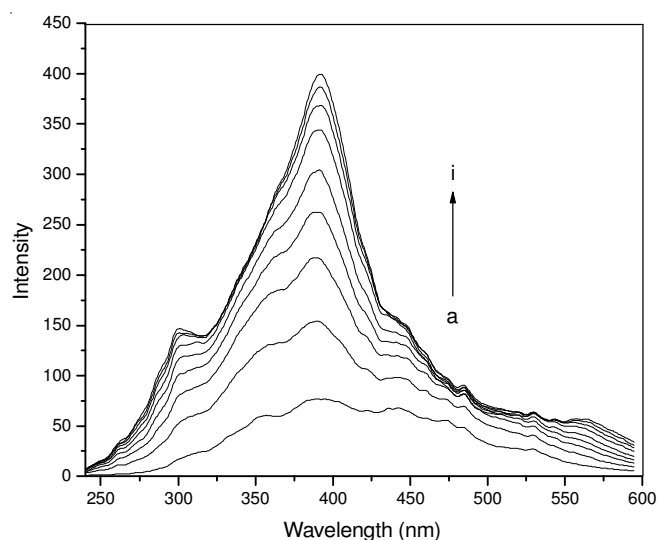


Fig. 6. Enhancement of resonance light scattering spectra of: lysozyme (2.5 μM) with various amounts of Congo red: 0 (a), 2.5 (b), 5 (c), 7.5 (d), 10 (e), 12.5 (f), 15 (g), 17.5 (h) and 20 μM (i), at pH 7.40

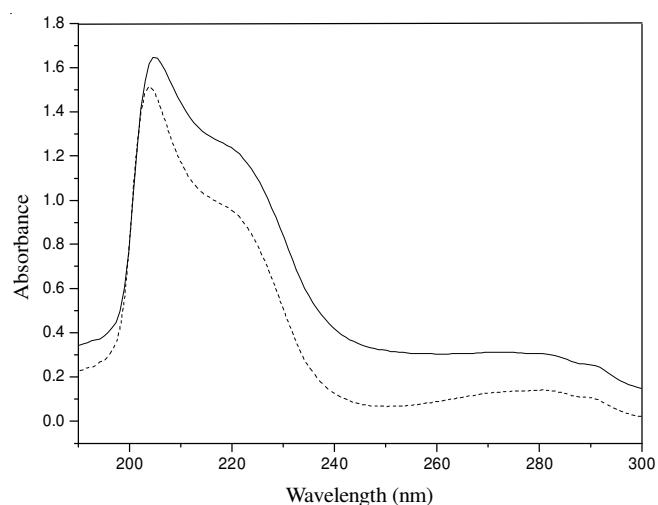


Fig. 7. Absorption spectra of lysozyme (2.5 μM) in the absence and presence of Congo red: Congo red/Lys molar ratio 0:1 (dot line) and 5:1 (solid line) at pH 7.40

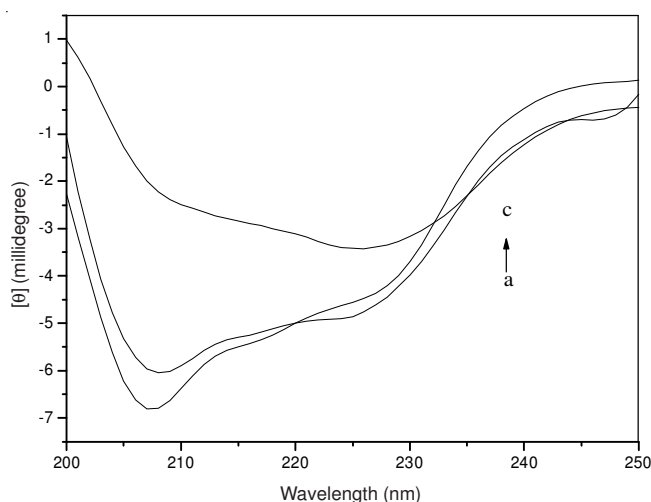


Fig. 8. CD spectra of: 6 μM lysozyme with various amount of Congo red: 0 (a), 12 (b) and 36 μM (c); at pH 7.40

Conclusion

The binding of Congo red with lysozyme may thus be summarized as follows. The contour plot of the fluorescence spectra provided the optimal excitation wavelengths for lysozyme and Congo red at 280 and 320 nm, respectively. The fluorescence of lysozyme is mainly originated from the tryptophan residues, which can be quenched by Congo red and the results showed that both static and dynamic quenching occurred together with complex formation. The interaction of Congo red with lysozyme was more than one binding sites with association constants of the order of 10^5 . Thermodynamic parameters for binding suggested that the interactions are primarily through hydrophobic interactions. The results of circular dichroism spectrum indicated that the secondary conformational changes of lysozyme upon interaction with Congo red. In addition, the data of resonance light scattering also indicated the changes of microenvironment of lysozyme induced by the binding Congo red.

ACKNOWLEDGEMENTS

This work was supported by the National Natural Science Foundation of China (No. 11105194), the Key Scientific Technology Research Project of Gansu Province (No. 092GKDA0033) and This work was supported by the Hundred Talent Program of the Chinese Academy of Science (O861010ZY0).

REFERENCES

1. B.P. Kamat and J. Seetharamappa, *Polish J. Chem.*, **78**, 723 (2004).
2. T.B. Tschopp, H.R. Baumgartner and A. Studer, *Thromb. Diath. Haemorrh.*, **26**, 488 (1971).
3. M. Giger, H.R. Baumgartner and G. Zbinden, *Agents Act.*, **4**, 173 (1974).
4. T.J. Haley, *Clin Toxicol.*, **8**, 13 (1975).
5. X. Zhang and J. Jin, *J. Mol. Struct.*, **882**, 96 (2008).
6. J. Jin and X. Zhang, *J. Lumin.*, **128**, 81 (2008).
7. T.V. Zenser, V.M. Lakshmi and B.B. Davis, *Drug. Metab. Dispos.*, **26**, 856 (1998).
8. A.R. Beaudoin, *Proc. Soc. Exp. Biol. Med.*, **117**, 176 (1964).
9. M. Tubis, W.H. Bland and R.A. Nordyke, *J. Am. Pharm. Assoc.*, **49**, 522 (1960).
10. C.J. Sheng and H.D. Dian, Lysozyme, Shandong Science and Technology Press, 50 (1982).
11. E. Pigorsch, A. Elhaddaoui and S. Turrell, *J. Mol. Struct.*, **348**, 61 (1995).
12. X.Z. Feng, Z. Lin, L.J. Yang and C. Wang, *Talanta*, **47**, 1223 (1998).
13. R.C. Lu, J.X. Xiao, A.N. Cao, L.H. Lai, B.Y. Zhu and G.X. Zhao, *Biochim. Biophys. Acta*, **1722**, 271 (2005).
14. C.Z. Huang, Y.E. Li and X.D. Liu, *Anal. Chim. Acta*, **375**, 89 (1998).
15. S. Deepa and A.K. Mishra, *J. Pharm. Biom. Anal.*, **38**, 556 (2005).
16. W.Y. He, Y. Li, C.X. Xue, Z.D. Hu, X.G. Chen and F.L. Sheng, *Bioorg. Med. Chem.*, **13**, 1837 (2005).
17. T.G. Dewey, Plenum Press, New York, pp. 1-41 (1991).
18. J.R. Lakowicz, Principles of Fluorescence Spectroscopy, Plenum Press, New York, pp. 266-7 (1983).
19. M.X. Xie, M. Long, Y. Liu, C. Qin and Y.D. Wang, *Biochim. Biophys. Acta*, **1760**, 1184 (2006).
20. A. Papadopoulou, R.J. Green and R.J. Frazier, *J. Agric. Food Chem.*, **53**, 158 (2005).
21. M.X. Xie, X.Y. Xu and Y.D. Wang, *Biochim. Biophys. Acta*, **1724**, 215 (2005).
22. P.D. Ross and S. Subramanian, *Biochemistry*, **20**, 3096 (1981).
23. N. Seedher, B. Singh and P. Sing, *Indian J. Pharm. Sci.*, **61**, 3 (2004).
24. F.L. Cui, J. Fan, J.P. Li and Z.D. Hu, *Bioorg. Med. Chem.*, **12**, 151 (2004).
25. Y.J. Hu, Y. Liu, J.B. Wang, X.H. Xiao and S.S. Qu, *J. Pharm. Biomed. Anal.*, **36**, 915 (2004).